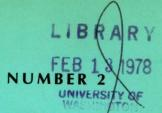
3 353:2

JANUARY 25, 1978 VOLUME 253



ISSN 0021-9258 JBCHA3 253(2) 319-645 (1978)

# THE Journalof Biological Chemistry

Published by The American Society of Biological Chemists, Inc.

FOUNDED BY CHRISTIAN A. HERTER

AND SUSTAINED IN PART BY THE CHRISTIAN A. HERTER MEMORIAL FUND



# **Biological Chemistry**

Copyright © 1978 by the American Society of Biological Chemists, Inc., 428 East Preston St., Baltimore, Md. 21202 U.S.A.

#### CONTENTS

### COMMUNICATIONS

- 319 Increase in hepatic tyrosine aminotransferase mRNA during enzyme induction by  $N^6$ ,  $O^2$ -dibutyryl cyclic AMP. Michael J. Ernest and Philip Feigelson
- 323 Use of the integrated steady state rate equation to investigate product inhibition of human red cell adenosine deaminase and its relevance to immune dysfunction.

  William R. A. Osborne, Shi-Han Chen, and C. Ronald Scott
- 326 Electrogenic behavior of synaptic vesicles from Torpedo californica.

  Richard S. Carpenter and Stanley M. Parsons
- 330 Specific adhesion of rat hepatocytes to β-galactosides linked to polyacrylamide gels. Paul H. Weigel, Eli Schmell, Yuan C. Lee, and Saul Roseman
- 334 Phosphorylation of cardiac troponin by guanosine 3':5'monophosphate-dependent protein kinase.

  Donald K. Blumenthal, James T. Stull, and Gordon N.
  Gill
- 337 Purified cyclic GMP-dependent protein kinase catalyzes the phosphorylation of cardiac troponin inhibitory subunit (TN-I). Thomas M. Lincoln and Jackie D. Corbin
- 340 Isolation and partial characterization of an endogenous inhibitor of ceramide glycosyltransferases from rat brain. Elvira Costantino-Ceccarini and Kunihiko Suzuki
- 343 Sequence homology of the Ca<sup>2+</sup>-dependent regulator of cyclic nucleotide phosphodiesterase from rat testis with other Ca<sup>2+</sup>-binding proteins.

  John R. Dedman, Richard L. Jackson, William E. Schreiber, and Anthony R. Means
- 347 Glycosaminoglycan sulfotransferases of the developing chick cornea.

  Gerald W. Hart
- 354 Effect of pressure and ionic strength on the self-association of apo-A-I from the human high density lipoprotein complex.
  Silvestro Formisano, H. Bryan Brewer, Jr., and James C. Osborne, Jr.
- 359 Appendix. Evaluation of volume changes in associating systems by sedimentation equilibrium. James C. Osborne, Jr.
- 361 Comparison of atypical and usual human serum cholinesterase. Purification, number of active sites, substrate affinity, and turnover number. Oksana Lockridge and Bert N. La Du
- 367 Mitochondrial ATPase activities of hepatoma BW7756 and ascites tumor cells. Influence of Mg<sup>2+</sup> ions, free fatty acids, and uncouplers.

  Randall L. Barbour and Samuel H. P. Chan
- 377 Human blood group glycosyltransferases. I. Purification of N-acetylgalactosaminyltransferase.

  Masako Nagai, Vibha Davè, Bruce E. Kaplan, and Akira Voebida.
- 380 Human blood group glycosyltransferase. II. Purification of galactosyltransferase.

  Masako Nagai, Vibha Davè, Helmut Muensch, and Akira Yoshida
- 382 Comparative studies of Hb Lepore Boston, Hb A<sub>2</sub>, and Hb A.

  Kazuhiko Adachi, Toshio Asakura, Frances M. Gill, and Elias Schwartz
- 385 Effects of divalent cations and nucleotides on the reactivity of the sulfhydryl groups of sarcoplasmic reticulum

- membranes. Evidence for structural changes occuduring the calcium transport cycle.

  Alexander J. Murphy
- Phosphodiesterase activator from rat kidney cortex. Gordon J. Strewler, Vincent C. Manganiello, and tha Vaughan
- Nucleotide sequence of rainbow trout (Salmo gaird ribosomal 5.8 S ribonucleic acid.

  Ross N. Nazar and Kenneth L. Roy
- 00 Transport of a nonphosphorylated nucleoside, 5'-d adenosine, by murine leukemia L1210 cells. David Kessel
- 404 Human erythrocyte 5'-AMP aminohydrolase. Purific and characterization. Shyun-long Yun and Clarence H. Suelter
- 409 Purification and properties of a third form of anth late-5-phosphoribosylpyrophosphate phosphorib transferase from the Enterobacteriaceae.

  Michael Largen, Stanley E. Mills, Joan Rowe, Charles Yanofsky
- 413 On the processive mechanism of Escherichia coli polymerase I. Quantitative assessment of processivi Robert A. Bambara, Dennis Uyemura, and The Choi
- 424 Processivity of DNA exonucleases.

  Kirk R. Thomas and Baldomero M. Olivera
- 430 Thioredoxin from Escherichia coli. Radioimmunolo and enzymatic determinations in wild type cells mutants defective in phage T7 DNA replication.

  Arne Holmgren, Ingrid Ohlsson, and Maja-Lena kvist
- 437 Enzymes for RNA sequence analysis. Preparation specificity of exoplasmodial ribonucleases I and II Physarum polycephalum.

  Daniel Pilly, Amanda Niemeyer, Maurice Schmidt J. Pierre Bargetzi
- 446 An induced aliphatic aldehyde dehydrogenase from bioluminescent bacterium, Beneckea harveyi. Pur tion and properties. Andrew L. Bognar and Edward A. Meighen
- 451 Intracytoplasmic membrane synthesis in synchronous populations of Rhodopseudomonas sphaeroides. Fe "old" and "new" membrane.

  Donald R. Lueking, Robert T. Fraley, and So Kaplan.
- 458 Intracytoplasmic membrane synthesis in synchronoupopulations of Rhodopseudomonas sphaeroides. peptide insertion into growing membrane.

  Robert T. Fraley, Donald R. Lueking, and Schaplan
- 465 Synthesis of photopigments and electron transport ponents in synchronous phototrophic cultures of R pseudomonas sphaeroides. Colin A. Wraight, Donald R. Lueking, Robert T. F and Samuel Kaplan
- 472 Biosynthesis of peptidoglycan. Definition of the mic vironment of undecaprenyl diphosphate-N-acetylomyl-(5-dimethylaminonaphthalene-1-sulfonyl) pentide by fluorescence spectroscopy. William A. Weppner and Francis C. Neuhaus
- 479 Identification of bound pyruvate essential for the acof phosphatidylserine decarboxylase of Escherichia Michel Satre and Eugene P. Kennedy
- 484 Independence of 1,25-dihydroxyvitamin D<sub>3</sub>-mediate cium transport from de novo RNA and protein synt Daniel D. Bikle, David T. Zolock, Robert L. Morr and Robert H. Herman

Full Instructions to Authors will be found in The Journal, 253, 1 (1978), and reprints may be obtained on request from the editorial



BIOEPIS EX 10



# Preliminary Refinement and Structural Analysis of the Fab Fragment from Human Immunoglobulin New at 2.0 Å Resolution\*

(Received for publication, July 7, 1977)

FREDERICK A. SAUL, L. MARIO AMZEL, AND ROBERTO J. POLJAK‡

From the Department of Biophysics, The Johns Hopkins University School of Medicine, Baltimore, Maryland 21205

The three-dimensional structure of the Fab fragment from human myeloma IgG New has been refined using "model building" and "real space" procedures. By these techniques, the correlation between the amino acid sequences and the 2.0 Å resolution multiple isomorphous replacement Fourier map has been optimized. The average shift of all atoms during real space refinement was 0.62 Å. A list of the refined atomic coordinates for the 440 amino acid residues in the structure is given. Ramachandran plots prepared using the refined coordinates show a distribution of  $\phi$ ,  $\psi$  angular values which corresponds to the predominant  $\beta$ -pleated sheet conformation present in the structure.

The structures of the homology subunits  $V_H$ ,  $V_L$ ,  $C_H 1$ , and  $C_L$  were superimposed by pairs and quantitatively compared. The closest similarities were observed between  $V_H$  and  $V_L$  and between  $C_H 1$  and  $C_L$ . Amino acid sequence alignments obtained from this structural superposition are given. The closest sequence homology in Fab New is observed between  $C_H 1$  ( $\gamma$  heavy chain) and  $C_L$  ( $\lambda$  light chain). In addition, there is considerable homology between the variable and constant regions.

The distances of close contacts between the homology subunits of Fab New have been determined. The closer contacts, those between atoms at a distance  $\leq 1.2$  times their van der Waals radii, are analyzed in relation to the constant, variable, and hypervariable nature of the immunoglobulin sequence positions at which they occur. Most of the residues which determine the closer contacts between  $V_{\rm H}$  and  $V_{\rm L}$  and between  $C_{\rm H}1$  and  $C_{\rm L}$  are structurally homologous and highly conserved or conservatively replaced in immunoglobulin sequences.

The relation between idiotypic determinants, antigen combining site and hypervariable regions, is discussed in terms of the refined model.

In this paper we present the results of a preliminary crystallographic refinement and a list of atomic coordinates of

\* This work was supported by Research Grant AI 08202 from the National Institutes of Health and by Research Grants NP-141B and IM-105C from the American Cancer Society. The costs of publication of this article were defrayed in part by the payment of page charges. This article must therefore be hereby marked "advertisement" in accordance with 18 U.S.C. Section 1734 solely to indicate this fact.

‡ Recipient of United States Public Health Service Research Career Development Award AI-70091. Fab New. Some features of the refined structure are discussed in relation to the genetic control and physiological function of immunoglobulins.

It is generally accepted (see review in Ref. 1) that electron density maps calculated by multiple isomorphous replacement techniques contain significant errors which may lead to imprecise determination of structural details such as the location of amino acid side chain atoms, bond angles,  $\phi$  and  $\psi$  values, *cis* or trans character of proline residues, etc. This refinement project was undertaken with the aim of obtaining more accurate coordinates which can be applied to structural studies of other immunoglobulins and Fab hapten complexes (2). The starting atomic coordinates were those of the structure previously described (3, 4) obtained using multiple isomorphous heavy atom replacements. Since the complete refinement of the structure of Fab New is a complex undertaking, we present here initial results obtained after application of two consecutive refinement techniques. In the first step we have applied a "model building" procedure (5) in which the measured atomic coordinates were adjusted to impose standard bond lengths and bond angles. In a second step a "real space" procedure (6, 7) was used to optimize the correlation between the Fab New model and the multiple isomorphous replacement, electron density Fourier map.

The coordinates obtained by these procedures have provided an improved model which has been used to compare the tertiary structure of the homology subunits, to calculate interatomic contacts that define the quaternary structure of Fab, and to re-examine the conformation of the combining site.

### METHODS

Measurement of Model Coordinates — Atomic coordinates were measured on the 2 Å (nominal) resolution model previously described (4). A two-pointer device was used for this purpose: a horizontal pointer (50 inches long) was brought to touch atom centers by displacing the device on the base of the model, adjusting the height of the pointer along a graduated scale (z coordinate) while a second, parallel, fixed pointer of equal length gave the x, y coordinates on a grid at the base of the model. The use of a level and leveling screws at the base of the two-pointer device was essential for obtaining reproducible coordinates. While these measurements were made, the image of the model and the atom centers were



<sup>&</sup>lt;sup>1</sup> The abbreviations used for immunoglobulins, their polypeptide chains, and fragments are as recommended in (1964) *Bull. W H O* 30, 447.

projected on the corresponding sections of the Fourier map using an optical comparator (8) to verify that their location and the coordinate

values corresponded with the Fourier map.

Model Building Procedure - The set of measured coordinates for the 3185 non-hydrogen atoms in the structure provided the starting point for this procedure. In general, these coordinates are subject to errors due to measurement uncertainty and to mechanical deformations of the skeletal brass model. Consequently, the mathematical model building procedure of Diamond (5) programmed for a digital computer was used in order to impose standard bond lengths and bond angles in the model. The measured coordinates were used to provide a guide point for each (non-hydrogen) atom in the structure. Some conditions used in this part of the refinement process are given in Table I. All the varied angles are dihedral; the  $\tau_{\alpha}(\tau_{N-C\alpha-C})$  angle was allowed to vary since this condition gave a much closer correlation with input coordinates without introducing large distortions in the idealized, model-built geometry of the molecule. Residues for which the model-built coordinates differed considerably from the input coordinates or which had an abnormal  $\tau_{\alpha}$  value were remeasured and checked for correspondence with the Fourier map. These discrepancies could always be traced to errors in the measurement of coordinates or to distortions of the brass model. When necessary the coordinates were measured again after rebuilding distorted regions and the remeasured coordinates were submitted to the model building procedure as guide points. The final average value of  $\Delta \tau_{\alpha}(\Delta \tau_{\alpha}=|\tau_{\alpha}-109.3^{\circ}|)$  for the 440 residues in the model-built structure was 5.43°. Pro 151 in CH1 was built and refined in the cis conformation. The root mean square shift from the initial coordinates for all non-hydrogen atoms in the structure was 0.2 Å

Real Space Refinement - The model-built coordinates were used as a starting set for real space refinement (6). The 2.0 Å electron density map used for the automatic fitting of the atomic coordinates was calculated using multiple isomorphous replacement phases as described before (3, 4). The electron density function was calculated at intervals of 1/160 along x, (a = 111.43 Å), 1/80 along y (b = 56.68)Å), and 1/130 along z (c = 90.30 Å) in sections of constant y. A computer program incorporating a fast-Fourier transform algorithm was used for this calculation. Five cycles of real space refinement were carried out using the conditions defined in Table II. Values of atomic radii for carbon, nitrogen, oxygen, and sulfur that gave fastest convergence in trials using a small part of the structure were adopted and kept constant during refinement. Progress in the refinement process was followed by inspection of the root mean square shifts in coordinates, shifts in the coordinates of individual atoms, and adjustments of amino acid scale factors. Unusually large shifts in coordinates were checked using the optical comparator and the Fourier map. All refinement calculations were carried out using computer programs implemented at the Brookhaven National Laboratories.

#### RESULTS AND DISCUSSION

The root mean square shifts of atomic coordinates after five cycles of real space refinement converged to an average value of 0.09 Å. The values after each cycle were: 0.46 Å, 0.20 Å, 0.13 Å, 0.10 Å, and 0.09 Å. The average shift of all atoms during real space refinement was 0.62 Å. In most parts of the molecule, the coordinates after refinement are in very good agreement with the features of the electron density map (Fig.

# Table I Conditions of model building refinement<sup>a</sup>

Parameters varied were:  $\phi$ ,  $\psi$ ,  $\chi$ ,  $\tau$ (N C $\alpha$  C). Flexible proline residues were used. In addition,  $\tau$ (C $\alpha$  C $\beta$  C $\gamma$ ) was allowed to vary in Cys, His, Phe, Trp, and Tyr residues. A list of the sources of the amino acid groups used in model building is given in Table I of Diamond (7).

Probe	Length (residues)	Filter constants	
		$\mathbf{C}_1$	$C_2$
1	1	0.1	10-4
2	2	0.1	$10^{-4}$ $10^{-4}$
3	3	0.1	$10^{-4}$

# Table II Conditions of real space refinement<sup>a</sup>

Zone length: 5 Margin width: 6 Fixed atomic radii: 1.4 Å

Relative atomic weights; C:6, O:7, N:8, S:16

Relative softness of angular parameters that were allowed to vary:

 $\phi$ ,  $\psi$ : 4.0  $\chi$ : 3.2 Filter levels:

 $\lambda_{\min}$   $\lambda_{\min}/\lambda_{\max}$  Scale factor and background 0.0001 0.01 Translational refinement 0.001 0.01 Rotational refinement 0.001 0.001

Electron density map grid; 111.43/160, 56.68/80, 90.30/130 along cell edges

1). Many carbonyl groups of the main polypeptide chain can be reliably positioned (Fig. 2). In general, coordinates of atoms in regions of strong, well defined electron density converged rapidly in the first cycle of refinement and moved very little in subsequent cycles. Atoms in regions of lower density converged more slowly. A few residues in poorly defined regions of low density showed little convergence, although their total shift from the starting coordinates was small. The movement of main chain atoms tended to be smaller than those of side chains, presumably due to their better defined electron density and to greater constraints on their positions.

The progress of refinement was checked after each cycle by inspecting the fit of atoms whose shifts were substantially greater than the average. Some side chain groups which had been shifted by the Diamond model building procedure were moved back to their original positions by real space refinement. In the fifth cycle of refinement, an average shift greater than 1 A occurred for three consecutive amino acid residues (Gly 166, Val 167, and His 168) in the C<sub>H</sub>1 region. Inspection of the position of these atoms showed that they had moved to a conformation that appears to be in better agreement with the electron density map than the original model. The coordinates for all atoms of Fab New after refinement, given in the "Appendix," are filed with the Protein Data Bank at Brookhaven National Laboratory. No major features of the map remain unexplained, although a number of possible solvent molecules are found on the surface of the molecule. The conventional R factor,2 based on Fc obtained with the coordinates in "Appendix" and an overall temperature factor (B =18.0), is R = 0.46. This value is reasonable given the refinement approximations outlined in Table II and the fact that no solvent atoms were included in the model. Further refinement using observed structure factors and calculated phases is currently underway.

The S—S distances in the five Fab disulfide bonds were allowed to vary without constraints. At the end of the refinement these distances were found to be:  $V_H$ , 2.00 Å;  $V_L$ , 2.46 Å;  $C_H$ 1, 2.30 Å;  $C_L$ 2, 2.30 Å;  $C_H$ 1- $C_L$ 2, 2.43 Å.

### Ramachandran Plots

The Ramachandran plots of the V<sub>L</sub> and C<sub>L</sub> homology sub-



<sup>&</sup>lt;sup>a</sup> See Diamond (6, 7) for definition of terms.

<sup>&</sup>lt;sup>b</sup> Nonlinear constraints were used to preserve chain continuity.

 $<sup>^2</sup>R = \Sigma |F_o - F_c|/\Sigma F_o$ , where  $F_o$  is observed structure amplitude and  $F_c$  is calculated structure amplitude.

<sup>&</sup>lt;sup>3</sup> The isotropic temperature factor (B) used in the expression exp

# DOCKET

# Explore Litigation Insights



Docket Alarm provides insights to develop a more informed litigation strategy and the peace of mind of knowing you're on top of things.

# **Real-Time Litigation Alerts**



Keep your litigation team up-to-date with **real-time** alerts and advanced team management tools built for the enterprise, all while greatly reducing PACER spend.

Our comprehensive service means we can handle Federal, State, and Administrative courts across the country.

## **Advanced Docket Research**



With over 230 million records, Docket Alarm's cloud-native docket research platform finds what other services can't. Coverage includes Federal, State, plus PTAB, TTAB, ITC and NLRB decisions, all in one place.

Identify arguments that have been successful in the past with full text, pinpoint searching. Link to case law cited within any court document via Fastcase.

# **Analytics At Your Fingertips**



Learn what happened the last time a particular judge, opposing counsel or company faced cases similar to yours.

Advanced out-of-the-box PTAB and TTAB analytics are always at your fingertips.

### API

Docket Alarm offers a powerful API (application programming interface) to developers that want to integrate case filings into their apps.

### **LAW FIRMS**

Build custom dashboards for your attorneys and clients with live data direct from the court.

Automate many repetitive legal tasks like conflict checks, document management, and marketing.

### **FINANCIAL INSTITUTIONS**

Litigation and bankruptcy checks for companies and debtors.

### **E-DISCOVERY AND LEGAL VENDORS**

Sync your system to PACER to automate legal marketing.

